

Applied Meteorology Unit (AMU) Quarterly Report

30 April 2012

Second Quarter FY-12

Contract NNK06MA70C



In this issue:

- Objective Lightning Probability Forecast, Phase IV**
- Objective Lightning Probability Forecasts for East-Central Florida Airports**
- Vandenberg AFB Upper-Level Wind Launch Weather Constraints**
- Assessing Upper-Level Winds on Day-of-Launch**
- Applications of Dual-Doppler Radar**
- Range-Specific High-Resolution Mesoscale Model Setup**

Launch Support

Dr. Bauman and Dr. Huddleston supported the Delta 4 launch on 19 January 2012.

Ms. Crawford, Ms. Shafer and Dr. Huddleston supported the Atlas 5 launch on 24 February 2012.

Atlas 5 launching the Navy's MUOS communication satellite on 24 February 2012
(<http://www.spaceflightnow.com/atlas/av030/launch/index2.html>)

This Quarter's Highlights

After over 40 years of serving the meteorological community, 20 of which were spent in the AMU, Mr. Mark Wheeler retired on March 30.

The AMU team worked on six tasks for their customers:

- Dr. Bauman and Ms. Crawford continued working on two objective lightning probability tasks, one for the Kennedy Space Center/Cape Canaveral Air Force Station (KSC/CCAFS) area and the other for airports in east-central Florida.
- Ms. Shafer created the first draft of a tool that will help Vandenberg Air Force Base forecasters determine the probability of violating specific upper-level wind criteria during launches.
- Dr. Bauman began developing a capability for the NASA Launch Services Program and 45th Weather Squadron to assess model forecasts of upper-level winds .
- Dr. Huddleston completed research to determine the feasibility of establishing a dual-Doppler capability using the 45th Space Wing and National Weather Service in Melbourne, Fla., radars.
- Dr. Watson continued testing high-resolution model configurations for the Eastern Range to provide forecasters with more accurate depictions of the future state of the atmosphere.



1980 N. Atlantic Ave., Suite 830
Cocoa Beach, FL 32931
(321) 783-9735, (321) 853-8203 (AMU)

Quarterly Task Summaries

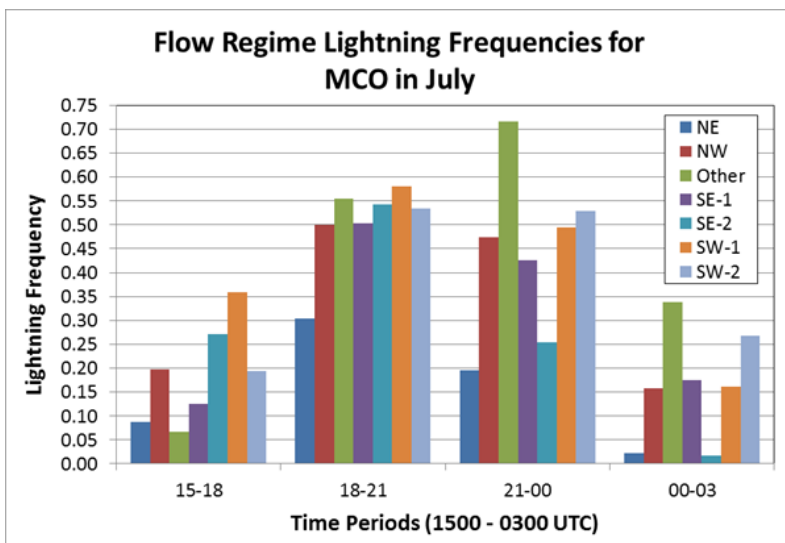
This section contains summaries of the AMU activities for the second quarter of Fiscal Year 2012 (January-March 2012). The accomplishments on each task are described in more detail in the body of the report starting on the page number next to the task name.

Objective Lightning Probability Forecast, Phase IV ([Page 4](#))

Purpose: Develop updated equations with six more years of data and use the National Lightning Detection Network (NLDN) daily lightning flash count across central Florida to determine if the data can be stratified by lightning sub-season instead of calendar month. If the data cannot be stratified by lightning sub-season, the monthly equations will be updated with the new data. The 45th Weather Squadron (45 WS) uses the AMU-developed Objective Lightning Probability tool as one input to their daily lightning forecasts. Updating the logistic regression equations with additional data and different stratifications could improve the lightning probability forecast and make the tool more useful to operations.

Accomplished: Created new lightning probability forecast equations and conducted tests to determine their performance compared to the equations currently used in 45 WS operations. The new equations did not outperform the current operational equations, so they will not be transitioned into operations. Updated the Meteorological Interactive Data Display System (MIDDS) graphical user interface (GUI) developed in Phase II with the October equation.

Objective Lightning Probability Forecasts for East-Central Florida Airports ([Page 7](#))



Purpose: Develop an objective lightning probability forecast tool for commercial airports in east-central Florida to help improve the lightning forecasts during the day in the warm season. The forecasters at the National Weather Service in Melbourne, Fla. (NWS MLB) are responsible for issuing forecasts for airfields in central Florida, and need to make more accurate lightning forecasts to help alleviate delays due to thunderstorms in the vicinity of an airport. The AMU will develop a forecast tool similar to that developed for the 45 WS in previous AMU tasks. The probabilities will be valid for the areas around the airports and time periods needed for the NWS MLB forecast.

Accomplished: Created and tested lightning probability forecast equations for Orlando International Airport (MCO) and determined their performance was not adequate. Met with NWS MLB forecasters to determine next steps.

Quarterly Task Summaries

(continued)

Vandenberg AFB Upper-Level Wind Launch Weather Constraints ([Page 10](#))

Purpose: Develop a tool to determine the probability of violating upper-level wind constraints to improve overall forecasts on the day of launch. This tool will allow the launch weather officers to evaluate upper-level thresholds for wind speed and wind shear constraints specific to Minuteman III ballistic missile operations at Vandenberg Air Force Base (VAFB).

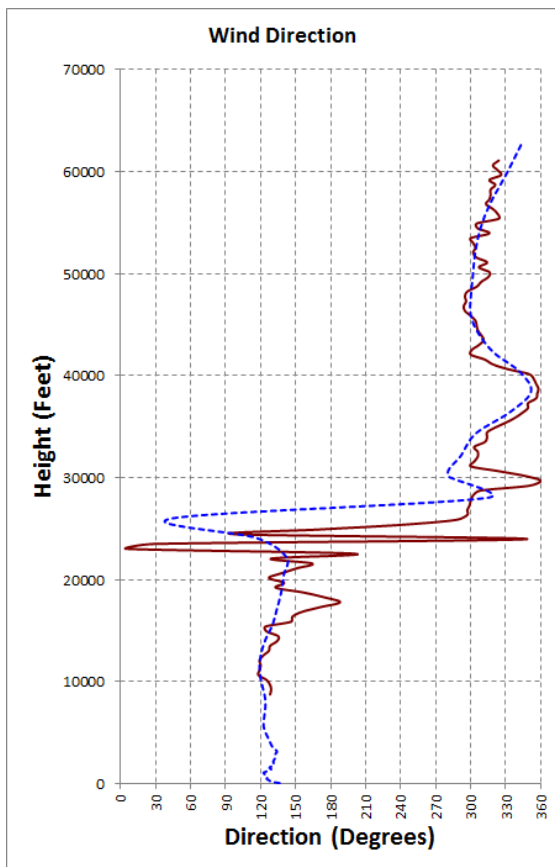
Accomplished: Completed processing the historical sounding data from the National Oceanic and Atmospheric Administration Earth System Research Laboratory (NOAA ESRL) and determined correct probability of violation (PoV) calculations for the wind speed and shear constraints. Continuing to develop the Excel GUI tool to display current sounding data and calculate the PoV for each launch constraint.



Assessing Upper-level Winds on Day-of-Launch ([Page 13](#))

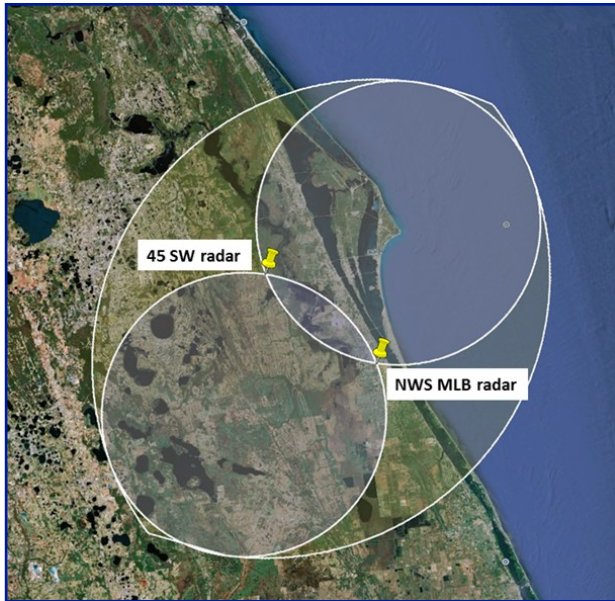
Purpose: Develop a MIDDs-based or Excel-based capability to rapidly assess the model forecast of upper-level winds by calculating the differences between model data and the current upper-level wind speed and direction observations from the 50 MHz Doppler Radar Wind Profiler and Automated Meteorological Profiling System (AMPS). This capability will provide an objective method for the Launch Weather Officers (LWOs) to compare the forecast upper-level winds to the observed data and assess the model potential to accurately forecast changes in the upper-level profile through the count.

Accomplished: Determined MIDDs does not have the model point data necessary, but the data are available for ingest through a PC to populate an Excel-based interface. Developed code in Excel to ingest and display 50 MHz profiler observations and model data.



Quarterly Task Summaries (continued)

Applications of Dual Doppler Radar ([Page 12](#))



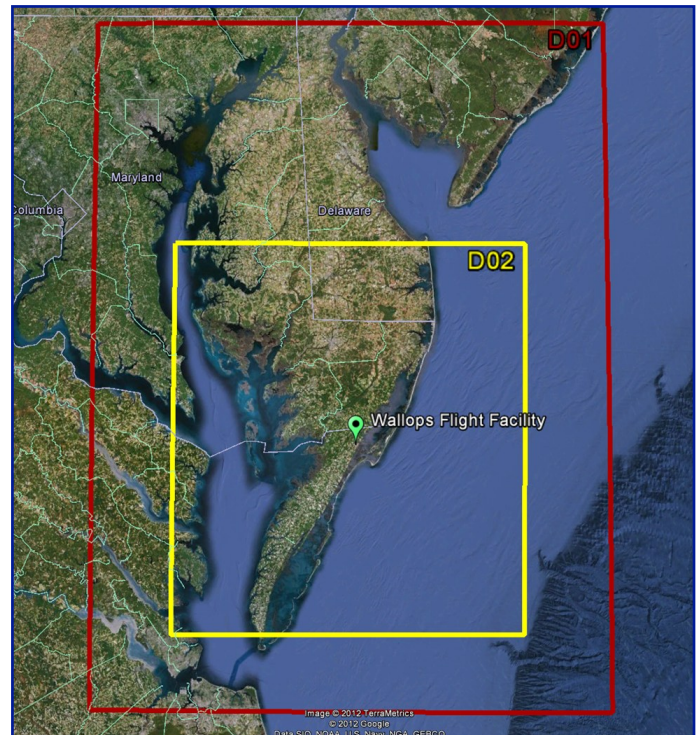
Purpose: Investigate the feasibility of creating a dual-Doppler capability using the 45 SW and NWS MLB Doppler radars. This would provide a three-dimensional display of the wind field and enhance the forecasters' ability to predict the onset of convection and severe weather. This task involves a literature review and consultation with experts to determine the requirements necessary to establish a dual-Doppler capability. Will also investigate cost considerations and viable alternatives.

Accomplished: Completed the geometry calculations of the dual-Doppler area encompassed by the 45 SW and NWS MLB radars. Completed investigating the project costs for the hardware and software involved in enabling the receipt of NWS MLB raw radar data in the Morrell Operations Center (MOC) for dual-Doppler synthesis. The final report was completed and after receiving NASA Scientific and Technical Information Program approval, was distributed and uploaded to the AMU website.

Range-Specific High-Resolution Mesoscale Model Setup ([Page 13](#))

Purpose: Establish a high-resolution model for the Eastern Range (ER) and Wallops Flight Facility (WFF) to better forecast a variety of unique weather phenomena. Global and national scale models cannot properly resolve important local-scale weather features due to their coarse horizontal resolutions. A properly tuned model at a high resolution would provide that capability and provide forecasters with more accurate depictions of the future state of the atmosphere.

Accomplished: Ran test cases for the warm and cool seasons using several Weather Research and Forecasting (WRF) model domain configurations. Results comparing the WRF model forecasts against wind tower, accumulated precipitation, and sounding data show that Advanced Research WRF (ARW) outperforms the WRF Non-hydrostatic Mesoscale Model (NMM), and that the ARW with the Lin microphysics scheme and Yonsei University planetary boundary layer scheme is the best configuration to use in real-time for the Eastern Range. Chose the grid configuration for WFF.



AMU ACCOMPLISHMENTS DURING THE PAST QUARTER

The progress being made in each task is provided in this section, organized by topic, with the primary AMU point of contact given at the end of the task discussion.

SHORT-TERM FORECAST IMPROVEMENT

Objective Lightning Probability Forecast – Phase IV (Dr. Bauman and Ms. Crawford)

The 45 WS includes the probability of lightning occurrence in their daily morning briefings. This forecast is important in the warm season months, May-October, when the area is most affected by lightning. The forecasters use this information when evaluating launch commit criteria (LCC) and planning for daily ground operations on Kennedy Space Center (KSC) and Cape Canaveral Air Force Station (CCAFS). The daily lightning probability forecast is based on the output from an objective lightning forecast tool developed in two phases by the AMU that the forecasters supplement with subjective analyses of model and observational data. The tool developed in Phase II consists of a set of equations, one for each warm season month, that calculates the probability of lightning occurrence for the day more accurately than previous forecast methods (Lambert and Wheeler 2005, Lambert 2007). The equations are accessed through a graphical user interface in the 45 WS primary weather analysis and display system, MIDDs. The goal of Phase III was to create equations based on the progression of the lightning season as seen in the daily climatology instead of an equation for each month in order to capture the physical attributes that contribute to thunderstorm formation. Five sub-seasons were discerned from the daily climatology, and the AMU created and tested an equation for

each. The Phase III equations did not outperform Phase II. Therefore, the Phase II equations are still in operational use. For this phase, the 45 WS requested the AMU make another attempt to stratify the data by lightning sub-season. The AMU did this by using lightning observations across central Florida from NLDN. After an extensive analysis, Dr. Bauman determined the NLDN-based lightning sub-seasons were unidentifiable, so he created monthly equations with six more years of data than used in Phase II. The new equations did not outperform those from Phase II and will not be transitioned to operations with the exception of the October equation that does not currently exist in the Phase II operational tool.

Predictors

Dr. Bauman used 12 stability and moisture parameters from the 1000 UTC CCAFS (XMR) soundings as candidate predictors in the equation development:

- Total Totals (TT),
- Cross Totals (CT),
- Vertical Totals (VT),
- K-Index (KI),
- Lifted Index (LI),
- Thompson Index (TI: KI – LI),
- Severe Weather ThrEAT (SWEAT) Index,
- Showalter Index (SI),
- Temperature at 500 mb (T_{500}),
- Mean Relative Humidity (RH) in the 825–525 mb layer,
- Mean RH in the 800–600 mb layer, and
- Precipitable Water up to 500 mb (PW).

These were added to the three predictors shown below, described in the AMU Quarterly Report Q4 FY06 and updated by Ms. Crawford using warm season data in the years 1989-2011, for a total of 15 candidate predictors:

- Daily climatological lightning frequency (Climo),
- 1-day persistence (Pers), and
- Flow regime lightning probability (FRProb).

New Equations

Dr. Bauman developed six new lightning probability forecast equations, one for each month May-October, using the development dataset that consisted of 19 warm seasons. He followed the same iterative procedure for choosing the predictors as outlined in Lambert and Wheeler (2005). The procedure involved adding one predictor at a time and checking the associated reduction in residual deviance. A large reduction in residual deviance meant that a predictor accounted for a large percentage of the variance in the predictand. Therefore, Dr. Bauman chose the predictors that effected the largest reduction. He stopped adding predictors as soon as a candidate predictor accounted for < 0.5% of the reduction in residual deviance.

Figure 1 shows the percent reduction in residual deviance from the NULL model as each predictor was added for the May equation. TI reduced the residual deviance the most (14.31%) and was, therefore, the first predictor in the May equation. The second predictor was Pers, which accounted for an additional 6.14% reduction. FRProb was the

third predictor, reducing the residual deviance by 4.42%. For May, Climo reduced the residual deviance by 0.26%, therefore, Climo was not chosen. The May equation consists of the predictors TI, Pers and FRProb.

Table 1 shows the final predictors for each of the monthly equations in rank order of their reduction in residual deviance. FRProb was the only predictor in all six months. The two strongest predictors in June, July, August and September were TI and FRProb, varying between first and second most important. FRProb and TI were also strong predictors in May but Pers was more important than FRProb. October is the outlier with LI and mean RH in the 800–600 mb layer as the top two predictors.

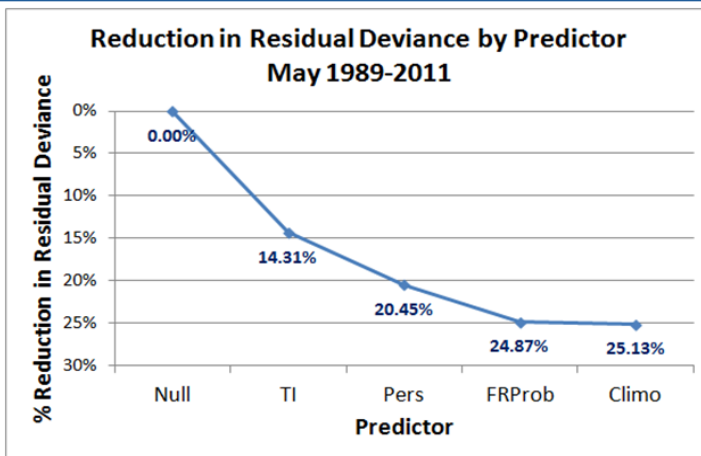


Figure 1. The total percent reduction in residual deviance from that of the NULL model as each predictor was added to the equation using the May development dataset.

Table 1. The final predictors for each monthly equation, in rank order of their contribution to the reduction in residual deviance. The predictors in red were in every equation, the predictors in blue were in five of the six equations, the predictors in green were in four of the six equations, the predictors in orange were in three of the six equations and the predictors in black were in two or less equations.

May	June	July	August	September	October
Thompson	Thompson	Flow Regime	Flow Regime	Thompson	Lifted Index
Persistence	Flow Regime	Thompson	Thompson	Flow Regime	825–600 RH
Flow Regime	825–525 RH	Total Totals	825–525 RH	Persistence	Flow Regime
	Persistence	Persistence	Total Totals		Total Totals
			Daily Climo		Daily Climo

in operations, hereafter designated as the operational equations.

Dr. Bauman calculated the percent improvement or degradation in skill of the new equations over the five forecast benchmarks using the Brier Skill Score (SS) defined in Wilks

Equation Testing

Dr. Bauman tested the performance of the equations using the verification dataset, which consisted of four warm seasons. None of the days in the verification set were contained in the development set to allow for an independent evaluation of performance. The first step was to determine if the new equations showed improvement in skill over five forecast benchmarks. Four of the benchmarks were the same as those in the Phase I task: Pers, Climo, FRProb, and monthly climatology. The fifth was the forecasts from the equations developed in Phase II of this work (Lambert 2007) and currently used

(2006) and Lambert (2007). The SS is positive when there is an improvement and negative when there is a degradation in skill. The SS values for each of the monthly equations are shown in Table 2. The predictors in the equations used to calculate the skill scores in Table 2 produced the best results with the verification dataset and were chosen using the method described in the previous section. The new equations showed a double-digit improvement in skill for the first four benchmarks in the table except for October daily climatology. For the individual months, May–September, the new equations show a degradation in skill compared to the

Table 2. The percent improvement (degradation) in skill of the new equations over the reference forecasts of persistence, daily and monthly climatologies, flow regime probabilities, and the operational equations developed in Lambert (2007). These scores were calculated using the verification data for each month.

Forecast Method	May	June	July	August	September	October
Persistence	52	48	48	59	37	37
Daily Climatology	31	16	10	17	14	7
Monthly Climatology	36	37	13	35	24	16
Flow Regime	34	35	12	34	12	16
Operational Equations	(-12)	3	(-2)	(-1)	(-19)	N/A

operational equations for May, July, August and September. The values of 3% for June, -2% for July and -1% for August are almost negligible and show similar skill between the new and operational equations for these months. Dr. Bauman created and tested equations with varying sets of predictors for the four months with a degradation in skill in an attempt to improve the skill of the new equations, but none was realized. Dr. Bauman discussed the results with Ms. Crawford and then Mr. Roeder of the 45 WS and all agreed not to transition the new May-September equations into operations.

MIDDS GUI

Dr. Bauman updated the MIDDS GUI developed in Phase II (Lambert 2007) with the October equation and delivered it to the 45 WS after testing to ensure proper performance. He modified the existing GUI using the Tool Command Language (Tcl)/Toolkit (Tk) capability in MIDDS.

The user accesses the GUI through the MIDDS Weather menu by clicking on the 'FCST Tools' button and choosing 'Lightning Forecast Tool' from the drop-down list (Figure 2). This activates the GUI Tcl/Tk code to determine the date and gather the appropriate data for the equation from MIDDS. The code checks the time and date of the most recent XMR sounding. If it does not match the current day and is not within the time period 0900–1159 UTC, an error message dialog box is displayed. This ensures that data from the previous day and data from sounding times other than 1000 UTC are not used in the equations. The 0900–1159 UTC period allows for the fact that not all 1000 UTC soundings are released precisely at 1000 UTC.

Whether or not the 1000 UTC XMR sounding for the current date is available, the equation predictor dialog box is displayed (Figure 3). This will allow the forecasters to use the GUI to create their seven-day forecasts even if data for the current day are not available. The dialog box has six tabs, one for each month. The tab of the current month is displayed initially if the GUI is run between May and October, otherwise 1 May is displayed. The current month, day and sounding time are printed along the top of the dialog box. If the current day's sounding is not available, 'No Current Sounding'

Figure 3. The predictor dialog box for October. A tab for each month is at the top, followed by the date and sounding time, then the predictor values. The 'Dismiss' button closes the GUI, the 'Reset Parameters' button resets the sounding parameters to the original values, and the 'Calculate Probability' button displays the probability output dialog box (Figure 4).

will be displayed in place of the date and time in the upper right. The day value can be changed by the up/down arrows or by entering a value manually in the text box. This allows forecasters flexibility when making the seven-day Weekly Planning Forecast. The sounding date and time is formatted by year, day of year, and UTC time.

Forecasters begin by choosing Yes or No for persistence, then a flow regime. They do not have to enter the sounding parameters as those values are already input by the GUI code and are displayed in their associated text boxes. If there is not a current sounding, the text boxes will be populated with the values from the most recent sounding available. The 'No Current Sounding'

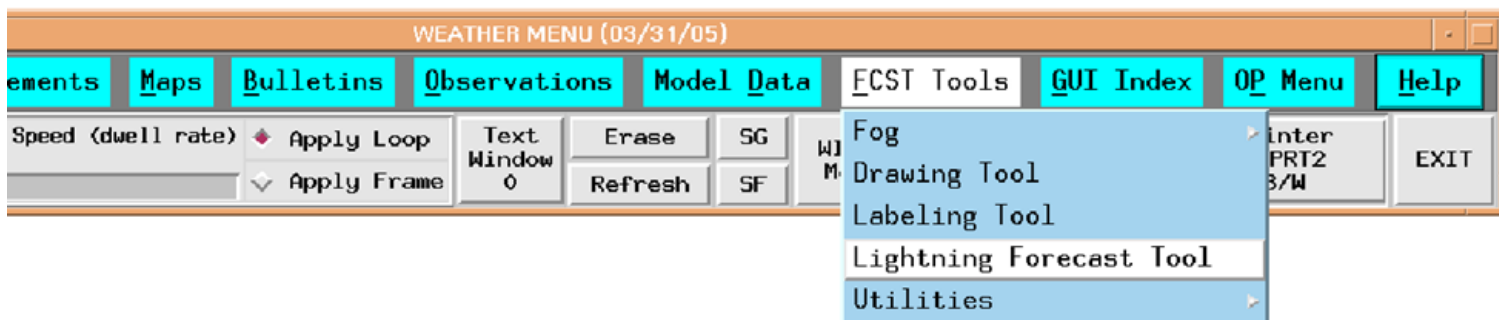


Figure 2. The MIDDS Weather Menu showing the FCST Tools button drop-down menu with Lightning Forecast Tool selected.

message in the top right corner will inform the forecaster that this is the case. If the routines cannot find a sounding file of any kind, the text boxes will be populated with the extreme low value in the range of available values for each sounding parameter.

The final step is to click on the 'Calculate Probability' button in the lower right corner of the dialog box. The 'Dismiss' button in the lower left closes the GUI. If the forecaster does not choose a persistence value or flow regime, an error message dialog box is displayed telling the forecaster to make a choice. There are separate error message dialog boxes for persistence and flow regime (not shown).

When the user clicks the 'Calculate Probability' button in the equation predictor dialog box, the probability of lightning occurrence for the day is displayed in a dialog box (Figure 4). The GUI code also outputs a file that contains all of the parameter values input by the user to calculate the probability. This file is currently named LtgProb.txt, and resides in the MIDDS data directory.

For more information contact Dr. Bauman at bauman.bill@ensco.com or 321-853-8202, or Ms. Crawford at crawford.winnie@ensco.com or 321-853-8130.

The probability of lightning being observed in at least one of the KSC/CCAFS advisory circles on Oct 1, from 0700 - 2400 EDT is:

1 %

OK

Figure 4. The output dialog box showing the probability of lightning occurrence for the day as calculated by the October equation with the values shown in the dialog box in Figure 3. The 'OK' button closes the box.

Objective Lightning Probability Forecasts for East-Central Florida Airports (Ms. Crawford and Dr. Bauman)

The forecasters at NWS MLB are responsible for issuing weather forecasts to several airfields in central Florida. They identified a need to make more accurate lightning forecasts to help alleviate delays due to thunderstorms in the vicinity of an airport. Such forecasts would also provide safer ground operations around terminals, and would be of value to Center Weather Service Units serving air traffic controllers in Florida. To improve the forecast, the AMU was tasked to develop an objective lightning probability forecast tool for the commercial airports in east-central Florida for which NWS MLB has forecast responsibility using data from the NLDN. The resulting forecast tool will be similar to that developed by the AMU for the 45 WS in previous tasks (Lambert and Wheeler 2005, Lambert 2007). The lightning probability forecasts will be valid for the time periods and area around each airport needed for the NWS MLB forecasts in the warm season months, defined as May-October.

Flow Regime Probabilities

After creating the predictand, the daily climatology and one-day persistence for equation development (AMU Quarterly Report Q1 FY12), Ms. Crawford calculated the monthly frequencies of lightning occurrence under each flow regime and in each 3-hour period at MCO, Melbourne International Airport and Space Coast Regional Airport in Titusville, Fla. She displayed the values in a Microsoft Excel PivotChart and sent the file to NWS MLB for their information and use. Figure 5 shows the flow regime lightning frequencies for July at MCO. In general, the values are low at the beginning of the day, increase through mid- to late-day, and decrease in the evening. This was the general trend for all months. The values for the 1800-2100 UTC time period in Figure 5 are similar. This could be due to MCO being closer to the

middle of the Florida land mass and being influenced by convection along the west and east coast sea breezes when the flow is westerly or easterly.

Equation Development and Testing

Ms. Crawford began equation development for MCO using the same iterative procedure for choosing the predictors as outlined in Lambert and Wheeler (2005) and the same development data set as in the Objective Lightning Probability Tool Phase IV task discussed previously. She created 24 equations, one for each month/time period combination and began testing them using the

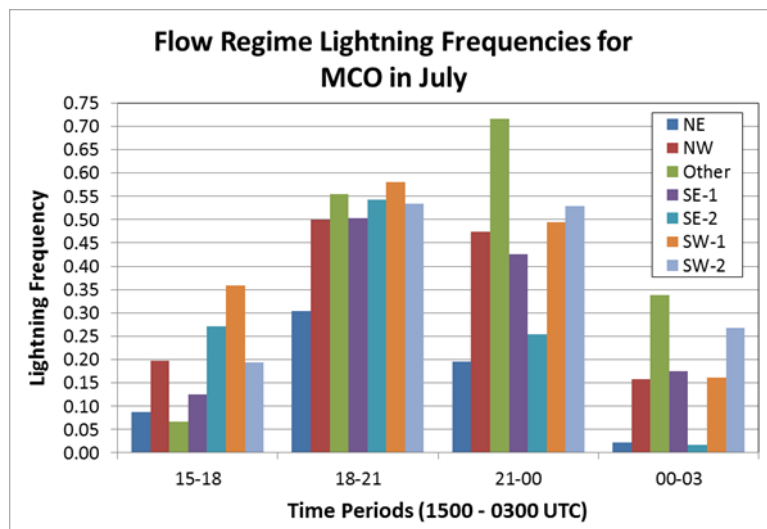


Figure 5. The frequency of lightning occurrence for each flow regime at MCO for the four 3-hour periods 1500-1800, 1800-2100, 2100-0000, and 0000-0300 UTC.

verification data set. She tested and refined the 24 MCO equations using SS values to determine performance compared to the daily climatology and flow regime probability values. Table 3 contains the SS values showing the skill of the MCO equations relative to the other forecast methods. Positive values indicate the equations had more skill than the corresponding forecast method, and negative values indicate less skill.

All equations outperformed 1-day persistence, but results for the daily climatology and flow regime probability were mixed. Values with magnitudes within 10% of 0, positive or negative, could indicate that the equations performed similarly to the corresponding forecast method. Out of the 72 values in the table, 30, or 42%, were in this category. These equations are meant to provide a good first guess when forecasters are determining the probability of lightning, but it appears that several of the equations would be ineffective in doing so.

Ms. Crawford analyzed the equations further by conducting a test to determine their ability to distinguish between lightning and non-lightning days. In order to have enough samples, she combined data from all months to evaluate each time period and data from all time periods to evaluate each month. Figure 6 shows the results for the four time periods. For good performance, the blue curves should have a maximum occurrence in the lower probability values decreasing to a minimum at higher probability values, and the red curves should have a minimum in the lower probability values increasing to a maximum at the higher values.

Table 3. The percent improvement (positive) or degradation (negative red font) in skill of the MCO equations over the forecast benchmarks of persistence, daily climatology and flow regime probabilities. These scores were calculated using the verification data set for each month. Cells shaded in yellow contain values within 10% of 0.

Month	Forecast Benchmark	15-18	18-21	21-00	00-03
May	1-Day Persistence	43	12	34	41
	Daily Climatology	13	25	7	1
	Flow Regime Probability	18	23	3	-4
June	1-Day Persistence	37	46	47	35
	Daily Climatology	10	18	24	8
	Flow Regime Probability	-2	12	14	7
July	1-Day Persistence	59	40	47	47
	Daily Climatology	5	1	3	10
	Flow Regime Probability	4	0	-2	0
August	1-Day Persistence	51	43	50	51
	Daily Climatology	11	22	23	4
	Flow Regime Probability	9	21	7	0
September	1-Day Persistence	43	50	47	48
	Daily Climatology	-3	4	15	6
	Flow Regime Probability	-4	-1	2	-2
October	1-Day Persistence	22	42	38	53
	Daily Climatology	-11	11	17	2
	Flow Regime Probability	-12	4	16	0

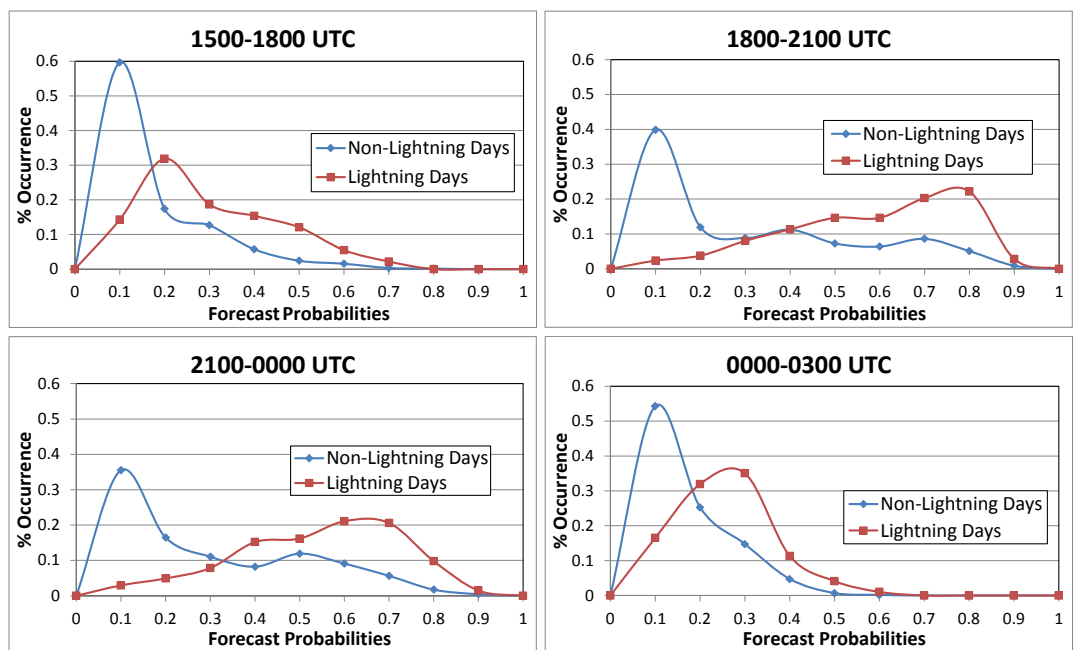


Figure 6. Forecast probability distributions for lightning (red) and non-lightning (blue) days in the verification data in each of the four time periods. The y-axis values are the frequency of occurrence of each probability value, and the x-axis values are the forecast probability values output by the equations.

The equations were able to distinguish non-lightning days in all periods, but performance was best in the 1500-1800 and 0000-0300 UTC periods at the beginning and end of the day. They were able to distinguish lightning days better in the afternoon time periods of 1800-2100 and 2100-0000 UTC than during 1500-1800 and 0000-0300 UTC. Still, the curves were spread over most of the range of forecast probabilities indicating ambiguous performance. The monthly values (not shown) revealed similar tendencies. May and October were similar to 1500-000 and 0000-0300 UTC, and June-September were similar to 1800-2100 and 2100-0000 UTC. These results were in agreement with the SS values in Table 3, indicating the equations would not provide a good first guess to the probability of lightning occurrence.

These results prompted Ms. Crawford to compare lightning occurrence in the development data set with that in the verification data set. A large percentage of lightning in one data set and a small percentage in the other could cause the bad performance seen in the SS values in Table 3 and the frequency distributions in Figure 6. Table 4 shows the percentage of lightning days in the development and verification data sets for each month and time period. The equations were developed with the development data and tested on the verification data. These values were calculated to determine if both data sets contained similar ratios of lightning to non-lightning days. That most values are within 4% indicates the data sets were similar with respect to lightning occurrence. The largest outlier of 9% occurred for July

Table 4. The percentage of lightning days in the development and verification data sets used to create and test the equations, respectively. The first column is the month, the second identifies the data set and the number of days it contains. The last four columns show the percentages of days with lightning in each time period.

<i>Month</i>	<i>Data Set (# Days)</i>	<i>15-18</i>	<i>18-21</i>	<i>21-00</i>	<i>00-03</i>
May	Development (544)	5	14	15	6
	Verification (107)	8	13	16	8
June	Development (521)	22	46	44	17
	Verification (109)	19	39	41	21
July	Development (530)	19	54	48	18
	Verification (121)	16	45	43	21
August	Development (526)	22	51	48	16
	Verification (115)	24	51	43	18
September	Development (509)	12	30	28	10
	Verification (113)	10	29	27	12
October	Development (494)	2	7	6	4
	Verification (101)	3	9	10	5

1800-2100 UTC. Note the low frequencies in May and October for all four time periods, and during 1500-1800 and 0000-0300 UTC for the other months. So few values make it difficult to determine strong relationships between the predictors and lightning occurrence.

Status

Ms. Crawford met with Mr. Volkmer and Mr. Sharp of NWS MLB in early April to discuss these results, and information she learned while attending Vaisala's International Lightning Meteorology Conference during the first week of April. NLDN underwent a major upgrade in 1994, causing researchers using the data to not use data before 1994. She spoke with Dr. Ken Cummins at the conference about NLDN detection

efficiencies (DE), resulting in him providing grids showing NLDN DEs over the U.S. during 1994-1998. Based on this information and the DE charts, they agreed to eliminate data in the years 1989-1994 from the data sets. This will require Ms. Crawford to create new development and verification data sets, daily climatology values and flow regime probabilities before creating new equations for MCO. She will also use the low-level mean speed combined with flow regime as a candidate predictor to determine if the combination has predictive ability for MCO.

For more information contact Ms. Crawford at 321-853-8130 or crawford.winnie@ensco.com, or Dr. Bauman at 321-853-8202 or bauman.bill@ensco.com.

Vandenberg AFB Upper-Level Wind Launch Weather Constraints (Ms. Shafer)

The 30th Weather Squadron (30 WS) provides comprehensive weather services to the space program at VAFB in California. One of their responsibilities is to monitor upper-level winds to ensure safe launch operations of the Minuteman III ballistic missile. The 30 WS tasked the AMU to analyze upper-level thresholds for wind speed and shear constraints specific to this launch vehicle using historical data collected at VAFB. The result will be a tool to assist the 30 WS forecasters in determining the climatological probability of exceeding specific wind threshold values, increase the accuracy of determining the PoV, and improve the overall forecast.

Data Processing

Ms. Shafer completed collecting the VAFB soundings from the NOAA ESRL database and modified existing scripts to import the sounding data into TIBCO Spotfire S+ (TIBCO 2010) for data analysis. She wrote a script to extract the sounding data needed for the task requirements and created monthly data files for the maximum wind speed and maximum 1000-ft shear constraints.

In order to determine the PoV for each wind constraint, the data needed to be interpolated to the 1000-ft height levels. Ms. Shafer wrote a Perl script to add the required levels to each sounding and interpolated the wind direction and speed to those 1000-ft heights. So that the PoV could be depicted accurately for the different times of the year and better represent the wind values, Ms. Shafer stratified the soundings into four sub-seasons: January-March, April-June, July-September and October-December. Ms. Shafer then determined the maximum wind speed and maximum 1000-ft shear val-

Variable Description	Formula
U-component wind	$U = Wspd \cdot \cos(270 - Wdir) \cdot \pi/180$
V-component wind	$V = Wspd \cdot \sin(270 - Wdir) \cdot \pi/180$
U-component shear	$U_{shear}(layer) = U(Upper) - U(Lower)$
V-component shear	$V_{shear}(layer) = V(Upper) - V(Lower)$
Shear of layer	$Shear(layer) = \sqrt{U_{shear}^2 + V_{shear}^2}$
Where: Wspd = Wind speed (knots) at given height. Wdir = Wind direction (degrees) at given height. Upper = top height (feet) of the layer of interest. Lower = bottom height (feet) of the layer of interest. $\pi = 3.14159265358979$	

ues for each sounding per sub-season. These values are necessary for determining statistics required to calculate the PoV per wind constraint. The 1000-ft layer shear values were calculated using the equations depicted in Table 5.

Data Distributions and PoV

To accurately calculate the PoV for each wind constraint Ms. Shafer determined the distribution of the maximum wind speed and maximum shear datasets. Dr. Merceret of the KSC Weather Office and Ms. Crawford assisted in this effort by determining which theoretical distributions fit the data. Ultimately they discovered the maximum wind speeds follow a Gaussian distribution while the maximum shear values follow a lognormal distribution. These results were applied when calculating the averages and standard deviations needed for the PoV calculations.

For the maximum wind speed PoV calculation, Ms. Shafer calculated the mean of the maximum wind speed values in each sounding within a given sub-season. She then cal-

culated the standard deviation of the same values. The results for each sub-season are shown in the second and third columns of Table 6. Since the distribution of the 1000-ft shear values was found to be lognormal, Ms. Shafer calculated the natural log (ln) of the maximum shear values and then the mean and standard deviation of the ln values to use in the PoV calculation. The results for each sub-season are shown in the fourth and fifth columns of Table 6.

Ms. Shafer then calculated the respective PoV values for each wind constraint per sub-season using the equations containing the MS Excel functions shown in Table 7. The "TRUE" option was selected to use the cumulative distribution function since it returns the probability of exceeding the variable constraint. The "FALSE" option would have returned a probability that the variable would be exactly equal to the constraint.

Excel GUI

The primary goal of this task is to develop a tool to determine the probability of violating upper-level wind

Sub-Season	Mean Max Wind Speed	Standard Deviation	Mean ln(Max Shear)	Standard Deviation
January-March	71.713	29.565	2.446	0.643
April-June	57.441	27.187	2.064	0.712
July-September	44.433	18.491	1.935	0.682
October-December	65.310	28.328	2.271	0.692

constraints specific to the Minuteman III ballistic missile launch vehicle at VAFB. Ms. Shafer developed this tool in Excel using Visual Basic to create a GUI that displays critical sounding data easily and instantly for the LWOs on the day of launch. Figure 7 shows the main page of the GUI with an example sounding loaded for display. The GUI consists of 12 data tabs; each with their own displays.

The “REVIEW” tab summarizes the launch constraint related sub-season and current sounding data. Once the LWOs click the “LOAD NEW BALLOON DATA” button, they should check the “CURRENT DISPLAYED BALLOON DATA” box to ensure the correct sounding is loaded into the GUI. To easily compare the current sounding to the climatology for the present sub-season, the “CURRENT SUB SEASON INFO” box displays the average maximum wind speed and 1000-ft shear values for the time period and the sub-season PoV of each wind constraint. The PoV results for each sub-season are shown in Table 7.

The “LAUNCH CONSTRAINTS AT A GLANCE” box focuses on the latest sounding data. It shows the maximum wind speed and its height, the maximum 1000-ft shear and its layer, and calculates the PoV for each constraint. Below the summary boxes are the “Maximum Wind Speed” and “Maximum 1000 ft Shear” graphs that display the current sounding data every 100-ft. The 30 WS requested that the 1000-ft shear be calculated at multiple intervals. For example, in addition to the 1000-2000-ft shear, the 1100-2100 ft, 1200-2200 ft, etc. values were also calculated. The “Maximum 1000-ft Shear” graph includes all of these calculations for the range of interest.

Sub-Season	Max Wind Speed	1000-ft Shear
January-March	1	7
April-June	0	3
July-September	0	2
October-December	0	5

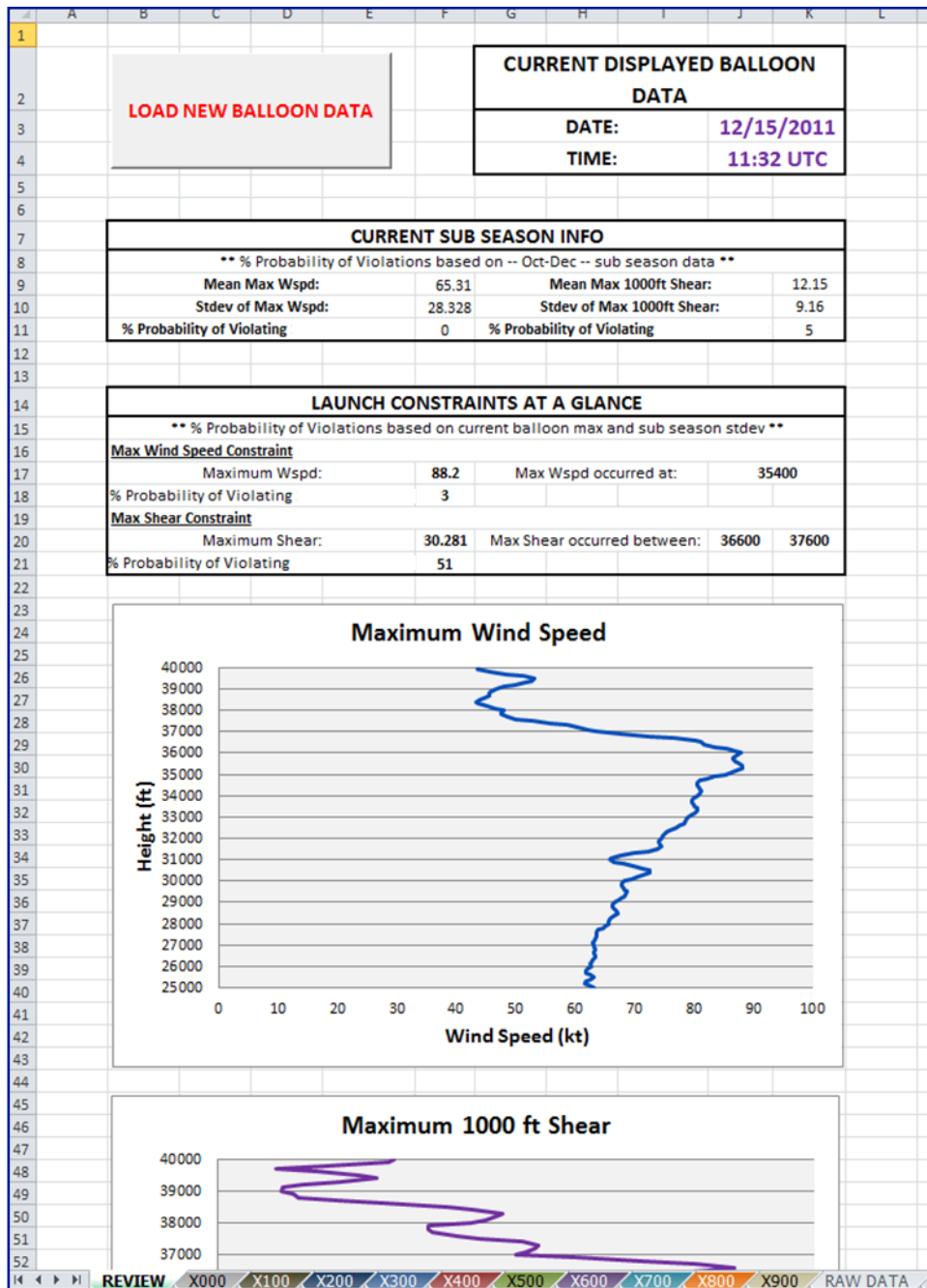


Figure 7. Screen shot of the 30 WS GUI display

The ten tabs labeled “X000”, “X100”, ... “X900” concentrate on the additional 100-ft interval shear levels. For example, “X100” includes the 25,100-26,100 ft, 26,100-27,100 ft, etc. heights. Each tab displays the sounding data at those heights, calculates the shear and then graphs the wind speed and shear values. The “RAW DATA” tab displays the latest raw data for the sounding loaded in the GUI.

Future Work

Ms. Shafer continues to develop the GUI that meets the requirements in the task plan. She delivered a preliminary version to Mr. Tyler Brock of the 30 WS for testing and comments. Based on conversations with Mr. Brock and Dr. Bauman, she is investigating adding model forecast data to overlay on the current sounding data. This will add predictive value for the LWOs on the day of launch.

Contact Ms. Shafer at 321-853-8200 or shafer.jaclyn@ensco.com for more information.

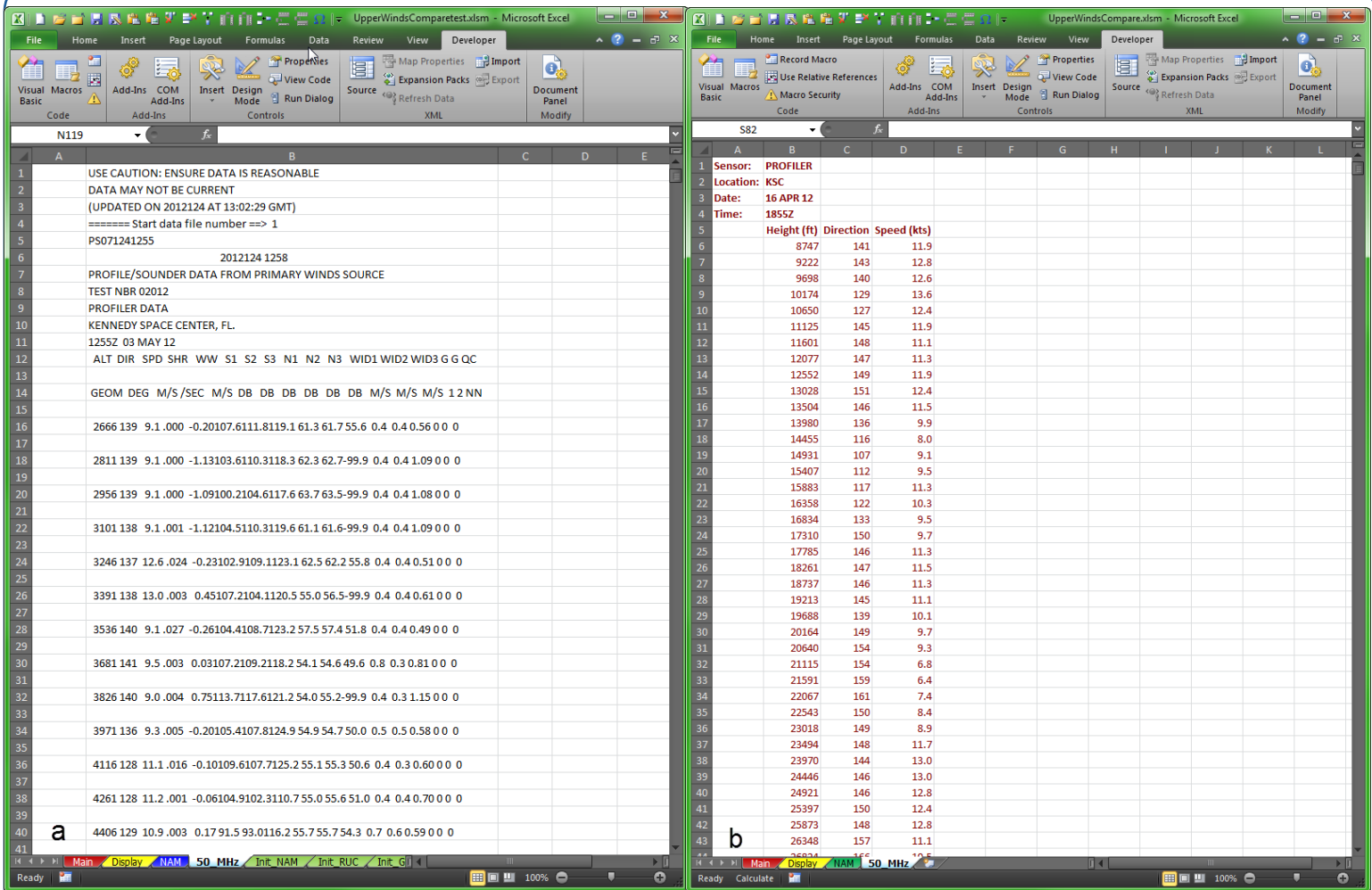


Figure 8. a) Data from the 50 MHz profiler after being ingested into Excel and b) after unneeded parameters were removed, displaying the sensor type and location, date, time, height, wind direction and speed.

Assessing Upper-level Winds on Day-of-Launch (Dr. Bauman)

On the day-of-launch, the 45th Weather Squadron (45 WS) launch weather officers (LWOs) monitor the upper-level winds for their launch customers to include NASA's Launch Services Program. They currently do not have the capability to display and overlay profiles of upper-level observations and numerical weather prediction model forecasts. The LWOs requested the AMU to develop a capability in the form of a GUI that will allow them to plot upper-level wind speed and direction observations from the KSC 50 MHz wind profiler and CCAFS AMPS radiosondes, and then overlay forecast profiles from the North American Mesoscale (NAM) model, Rapid Update Cycle (RUC) model and Global Forecast

System (GFS) model to assess the performance of these models.

Data Availability

Mr. Wheeler reviewed the availability of the observational and model data in MIDDS. He determined that the current MIDDS cannot be used as the data ingest and display for this task because the model point data is not ingested by MIDDS. To use Excel, Mr. Wheeler verified the observational data are available on the Spaceport Weather Data Archive at KSC (<http://trmm.ksc.nasa.gov/>). The archive consists of all locally collected weather data at KSC and CCAFS. He also located the model point data for CCAFS (XMR) at the Iowa State University Archive Data Server (<http://mtarchive.geol.iastate.edu>) in a format that can be ingested into Excel. After discussing this with the 45 WS, all agreed that the AMU

would develop an Excel GUI with data from these two external servers.

Excel GUI

Dr. Bauman developed code in Excel Visual Basic for Applications (VBA) to ingest and format the 50 MHz profiler data from the Spaceport Weather Data Archive. The data files are in American Standard Code for Information Interchange (ASCII) format and were ingested into Excel as a text file as shown in Figure 8a. After downloading and ingesting the data files, the VBA code removes all unneeded parameters and reformats the profiler data as shown in Figure 8b. From the reformatted data, the next VBA script creates wind speed and direction profile charts.

Dr. Bauman then wrote a VBA script to download and process the NAM model data from the Iowa State University server. The data files are in ASCII format and were ingested

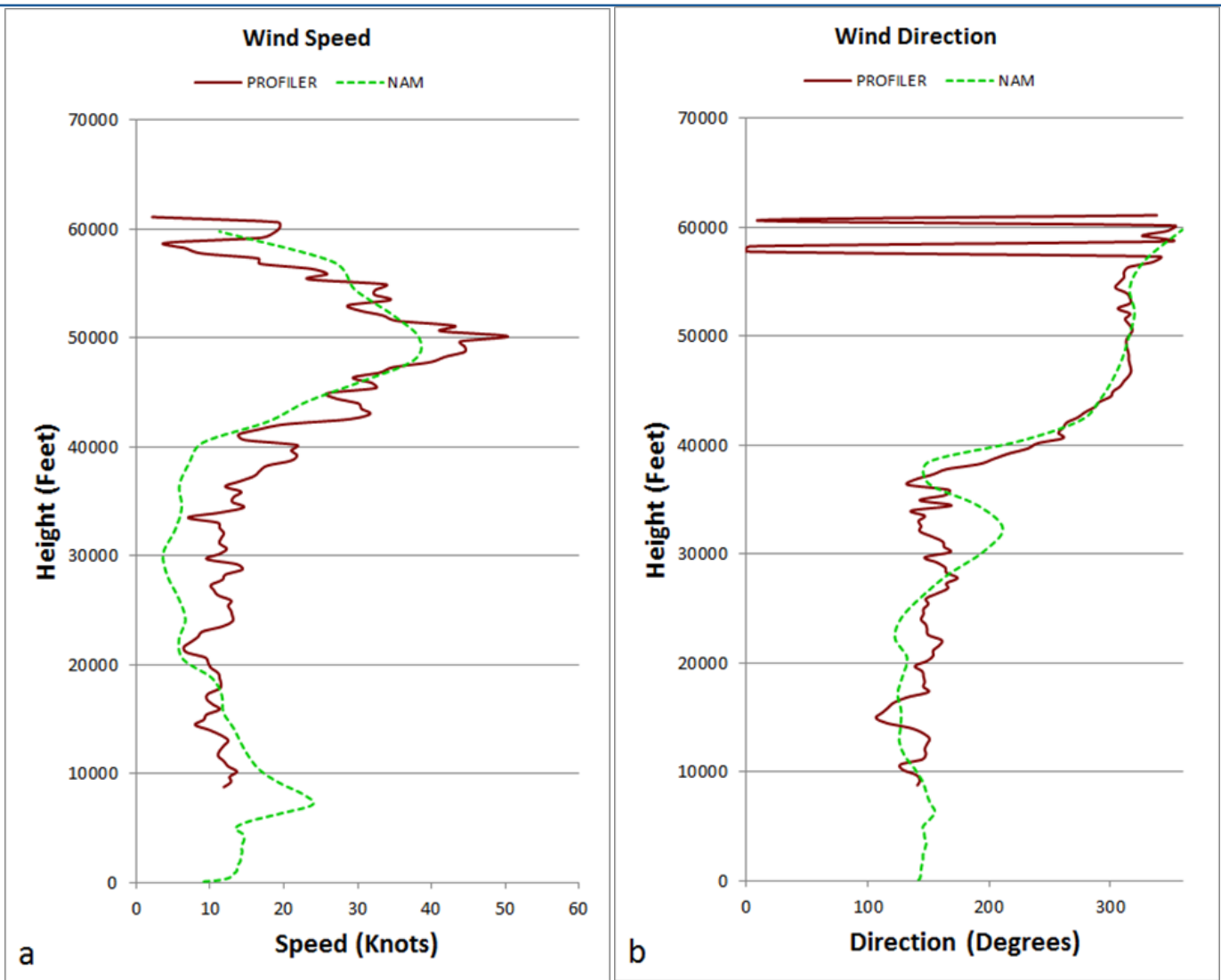


Figure 9. Wind speed (a) and wind direction (b) profiles from the 50 MHz profiler (solid dark red lines) and the NAM model point data forecast (dashed green lines) plotted in Excel.

into Excel as text files. The script reformats the file and displays the tabular data. From the reformatted data, the next VBA script creates wind speed and direction profiles of the NAM point data forecast and overlays the plots on the 50 MHz profiler charts as shown in Figures 9a

and 9b, respectively. Note that the lowest height available from the 50 MHz profiler is 8747 ft.

Next, Dr. Bauman will develop VBA scripts to download, ingest and process the AMPS wind speed and direction observations, RUC model and GFS model data.

For more information contact Dr. Bauman at bauman.bill@ensco.com or 321-853-8202.

INSTRUMENTATION AND MEASUREMENT

Applications of Dual-Doppler Radar (Dr. Huddleston)

When two or more Doppler radar systems are monitoring the same region, the Doppler velocities can be combined to form a three-dimensional wind vector field. Such a wind field allows a more intuitive

analysis of the airflow, especially for users with little or no experience in deciphering Doppler velocities (Bousquet, 2004). A real-time display of the wind field could assist forecasters in predicting the onset of convection and severe weather. The data could also be used to initialize local numerical weather models. Two Doppler radars are in the vicinity of KSC and CCAFS: the 45th Space Wing

(45 SW) RadTec 43/250 radar and NWS MLB Weather Surveillance Radar 1988 Doppler (WSR-88D). The 45 WS, NWS MLB and NASA customers tasked the AMU to investigate the feasibility of establishing dual-Doppler capability using these two systems. This task consisted of a literature review and consultation with experts to determine geometry, methods, techniques, hardware and

software requirements necessary to create a dual-Doppler capability. The AMU also investigated cost considerations and viable alternatives.

Dual-Doppler Area

The locations and resulting beam crossing angles of the 45 SW and NWS MLB radars make them ideally suited for a dual-Doppler capability. The total coverage area consists of the intersection between the areas within two dual-Doppler lobes defined by the upper limits on velocity error variance, and a football shaped area defined by the maximum range of the radars. The dual-Doppler total coverage area for the 45 SW and NWS MLB radars is shown in Figure 10. Dr. Huddleston provided a description of how she determined these areas in the previous AMU Quarterly Report (Q1 FY12).

Hardware and Software

There are several options to collect, edit, synthesize and display dual-Doppler data sets. The 45 SW currently uses the Interactive Radar Information System (IRIS™) software by Vaisala to display their radar data. The IRIS™ software has an add-on product called NDOP that can ingest WSR-88D data and provide the capability to calculate Dual-Doppler wind fields based on radial wind inputs from two Doppler radars. An example of an IRIS™ NDOP product display is shown in Figure 11. Ingesting data from two radars also provides the opportunity to eliminate the cone of silence, an important issue for thunderstorms approaching from the west or southwest, a frequent trajectory in the summer. The license includes the ability to make mosaics, or composites, of radar products from multiple sites. The list cost is \$16,000. This is a one-time cost for an add-on license to the existing IRIS software used by the 45 WS. Also a variety of freeware packages are available from the National Center for Atmospheric Research for processing raw radar data, but these packages do not have the thorough documentation and stringent configuration control needed in order to be certified for 45 WS use.

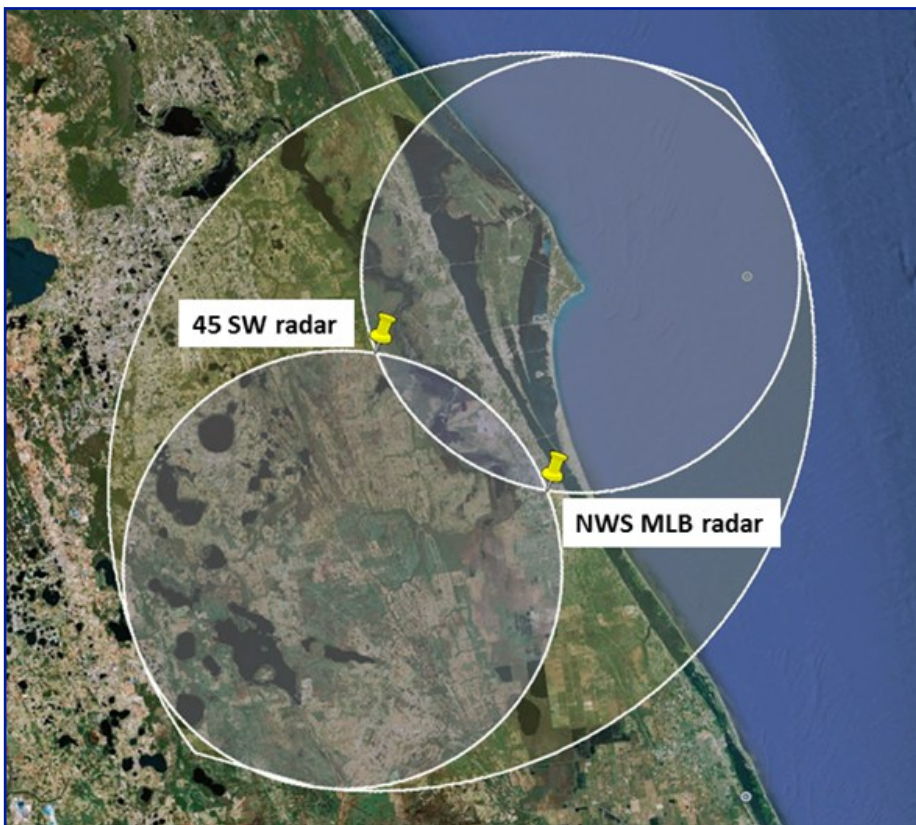


Figure 10. The total coverage area for the 45 SW and NWS MLB radars. The yellow pins show the locations of the radars.

Regardless of software choice, a T1 data line must be installed between the MOC on CCAFS and NWS MLB to enable the receipt of NWS MLB raw radar data needed for the dual-Doppler synthesis. This line, with additional costs, could also be used to send the 45 SW radar data to NWS MLB. In this case, NWS MLB can use the multi-sensor, multi-radar processing options via the Warning Decision Support System Integrated Information (WDSS-II) system for viewing the dual-Doppler radar data and then pass this information back to the 45 WS. The AMU could then create a way to view the dual-Doppler data using Meteorological Interactive Data Display System (MIDDs), Advanced Weather Interactive Processing

System (AWIPS), or other display techniques. Due to the proprietary nature of the vendor costs of in-

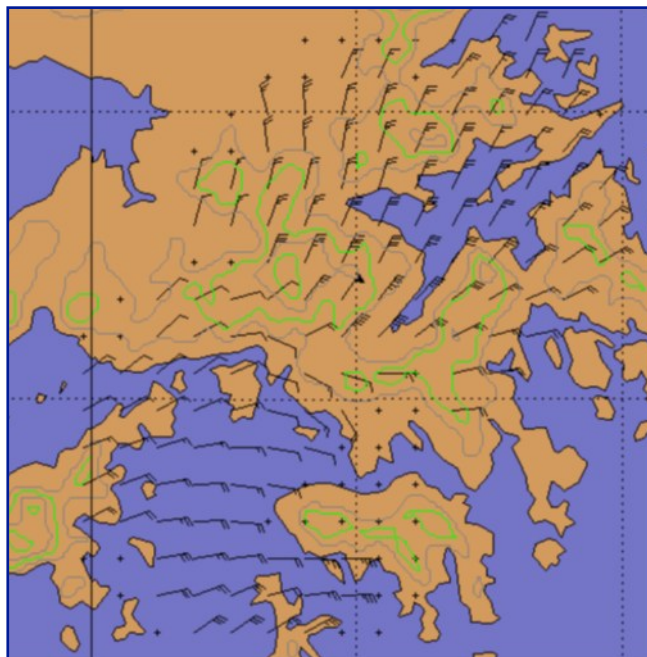


Figure 11. An example of an NDOP Display for strong northerly winter monsoon flow over China near Hong Kong, colliding with easterlies over the sea. The “+” points show regions where the minimum crossing angle between radars was met, but there were no weather targets, so a wind could not be calculated. The green and gray contours indicate ~300 m (~1000 ft) elevation intervals (Vaisala IRIS™ Product and Display Manual 2006).

stalling and maintaining the T1 line, performing drawing and configuration changes, and assuring information security functions, the 45 WS could only provide a lower bound on the cost. The cost and time estimate given for this project was a minimum of \$150,000 and 6 to 12 months to

complete. A monthly maintenance cost of the T1 line was estimated to be \$1000.

Status

Dr. Huddleston completed the final report after making modifications suggested in the internal AMU

and external customer reviews. The final report has been distributed to customers and uploaded to the AMU website.

For more information contact Dr. Lisa Huddleston at 321-853-8217 or lisa.l.huddleston@nasa.gov.

MESOSCALE MODELING

Range-Specific High-Resolution Mesoscale Model Setup (Dr. Watson)

The ER and WFF would benefit greatly from high-resolution mesoscale model output to better forecast a variety of unique weather phenomena. Global and national scale models cannot properly resolve important local-scale weather features at each location due to their horizontal resolutions being much too coarse. A properly tuned model at a high resolution would provide that capability. This is the first phase in a multi-phase study in which the WRF model will be tuned individually for each range. The goal of this phase is to tune the WRF model based on the best model resolution and run time while using reasonable computing capabilities. The ER and WFF supported tasking the AMU to perform a number of sensitivity tests in order to determine the best model configuration for operational use at each of the ranges.

ER Grid Configuration

Dr. Watson reassessed the results from the two WRF NMM configurations evaluated in the prior AMU Quarterly Report (Q1 FY12) and decided to compare them to results from the ARW core. She first compared the following configurations:

- Configuration 1: NMM core, 3 km outer domain and 1 km inner domain, Ferrier microphysics scheme, Mellor-Yamada-Janjic (MYJ) planetary boundary layer (PBL) scheme (NMM 3/1),

- Configuration 2: NMM core, 2 km outer domain and 0.67 km inner domain, Ferrier microphysics scheme, MYJ PBL scheme (NMM 2/0.6), and
- Configuration 3: ARW core, 2 km outer domain and 0.67 km inner domain, Lin microphysics scheme, Yonsei University PBL scheme (Lin-Yonsei).

Dr. Watson ran test cases for all three configurations for August 2011. She ran a 9-hour forecast once per day starting at 1500 UTC using the 12-km North American Mesoscale (NAM) model for boundary and initial conditions. Dr. Watson chose the initial time and run duration in order to capture the sea breeze in the warm season. She found that the ARW configuration produced a better overall forecast than the two NMM configurations. Detailed results are given in the next section. Based on those findings, Dr. Watson decided to run the ARW model with different physics options and compared the results of eight different configurations including Configuration 3:

- Configuration 4: ARW core, 2 km outer domain and 0.67 km inner domain, Ferrier microphysics scheme, Yonsei University PBL scheme (Ferrier-Yonsei),
- Configuration 5: ARW core, 2 km outer domain and 0.67 km inner domain, WDM6 microphysics scheme, Yonsei University PBL scheme (WDM6-Yonsei),
- Configuration 6: ARW core, 2 km outer domain and 0.67 km inner domain, Goddard microphysics scheme, Yonsei University PBL scheme (Goddard-Yonsei),

- Configuration 7: ARW core, 2 km outer domain and 0.67 km inner domain, Ferrier microphysics scheme, Mellor-Yamada-Janjic PBL scheme (Ferrier-MYJ),
- Configuration 8: ARW core, 2 km outer domain and 0.67 km inner domain, WDM6 microphysics scheme, Mellor-Yamada-Janjic PBL scheme (WDM6-MYJ),
- Configuration 9: ARW core, 2 km outer domain and 0.67 km inner domain, Ferrier microphysics scheme, NCEP Global Forecast System (GFS) PBL scheme (Ferrier-GFS), and
- Configuration 10: ARW core, 2 km outer domain and 0.67 km inner domain, WDM6 microphysics scheme, NCEP GFS PBL scheme (WDM6-GFS).

Due to time constraints, Dr. Watson compared a 9-hour forecast run once per day at 1500 UTC for August 1-7, 2011 instead of the whole month. She used the 12-km NAM model for boundary and initial conditions. In both ARW runs that used the GFS PBL scheme, the 2 m shelter temperatures routinely increased to unrealistic values of over 100 °F. Therefore, Dr. Watson dropped both Configuration 9 and 10 from the comparison.

Warm Season Results

All results described in this section compare the forecast values from the inner domain of the specified configurations. Dr. Watson validated the WRF model forecasts with data from seven KSC/CCAFS wind towers. She computed the monthly bias and root mean square error for

wind speed, direction, temperature and dewpoint temperature for Configurations 1-3 at select towers during August 2011. The WRF ARW configuration performed better overall than the NMM configurations. Based on those findings, Dr. Watson validated the WRF ARW Configurations 3-8 forecasts with data from the KSC/CCAFS wind towers. Table 8 shows results for wind direction, wind speed, temperature, and dewpoint temperature bias for August 1-7, 2011 for all configurations. In general, Lin-Yonsei (3), Ferrier-Yonsei (4) and Goddard-Yonsei (6) forecast wind speed and direction best while WDM6-MYJ (8) and NMM 2/0.6 (2) performed the best for temperature and dewpoint temperature forecasts, respectively.

Dr. Watson compared the 9-hour forecast accumulated rainfall from Configurations 1-3 to the 9-hour accumulation of observed rainfall using the National Centers for Environmental Prediction (NCEP) Stage-II analysis data (<http://www.emc.ncep.noaa.gov/mmb/ylin/pccpan/stage2/>). Results indicated that the ARW configuration outperformed both NMM configurations.

Dr. Watson validated the six ARW configurations against the daily 2200 UTC XMR sounding. She computed the mean error for wind direction, wind speed, temperature, and dewpoint temperature (Table 9). Bold green values indicate the best performing models for each forecast variable. Overall, both Lin-Yonsei (3) and Ferrier-Yonsei (4) performed the best.

Cool Season Results

Based on the results from the warm season model runs, Dr. Watson chose to compare the Ferrier-Yonsei, Lin-Yonsei, and NMM 3/1 configurations in the cool season. Both Lin-Yonsei and Ferrier-Yonsei performed consistently well, while NMM 3/1 was included to determine if the NMM performed better in the cool season. She ran test cases for the three configurations for the eight days February 18-25, 2012. She produced 9-hour fore-

Table 8. Mean error of wind speed (m/s), direction (deg), temperature (°F), and dewpoint temperature (°F) from 1-7 August 2011 for all configurations. Bold green values indicate the best performing model and bold red values indicate the worst performing model.

Configuration Name (#)	Wind Dir	Wind Spd	Temp	Dewpt
NMM 3/1 (1)	47	1.0	-1.5	0.7
NMM 2/0.6 (2)	50	0.8	-2.2	-0.1
Lin-Yonsei (3)	47	-0.1	-0.9	-2.0
Ferrier-Yonsei (4)	46	0.1	-1.1	-1.8
WDM6-Yonsei (5)	50	0.0	-1.1	-2.3
Goddard-Yonsei (6)	48	0.0	-1.1	-2.0
Ferrier-MYJ (7)	48	1.3	-1.0	-1.6
WDM6-MYJ (8)	49	1.0	-0.6	-1.8

casts twice per day starting at 0000 and 1200 UTC using the 12-km NAM model for boundary and initial conditions, Short-term Prediction Research and Transition Center (SPoRT) Land Information System land surface data, and SPoRT sea surface temperature data. Dr. Watson chose these initial times to capture as much of the day and night as possible.

Data for towers 511, 512, and 513 were not available between February 18-25, 2012, so Dr. Watson validated results from the cool season forecasts using towers 2, 6, 108, and 110. Both ARW configuration runs forecast nearly identical values for wind direction, wind speed, temperature and dewpoint temperature and slightly outperformed the NMM run. None of the configurations outperformed the other in forecasting precipitation in the cool season. Results against sounding data were not evaluated since the data were only available at 1100 and 2300 UTC, which did not occur within the 9-hour 0000 or 1200 UTC forecast periods.

Additional Comparison

Dr. Watson compared two Lin-Yonsei configurations for August 1-7, 2011 with varying horizontal grid spacing to determine if a slightly coarser resolution would have much impact on the results. The first configuration had a 2 km outer domain and a 0.67 km inner domain, and the second had a 3 km outer and 1 km inner domain. The mean error for wind direction, wind speed, temperature and dewpoint temperature were computed for each configuration at select towers. Results are shown in Table 10. The first number indicates the forecast value from the 2/0.67 km configuration and the second is from the 3/1 km configuration. Bold green values indicate the best performing model for each forecast variable. The results are nearly the same for both the wind speed and dewpoint temperature. The Lin-Yonsei 3/1 km outperformed the 2/0.67 km for wind direction while the 2/0.67 km was better for forecasting temperature.

Table 9. Mean error of wind speed (m/s), direction (deg), temperature (°F), and dewpoint temperature (°F) for the 2200 UTC XMR sounding from August, 1-7 2011 for the six ARW configurations. Bold green values indicate the best performing model(s) for each forecast variable.

Configuration Name (#)	Wind Dir	Wind Spd	Temp	Dewpt
Lin-Yonsei (3)	35	-0.1	0.4	-5.5
Ferrier-Yonsei (4)	38	0.0	0.4	-4.8
WDM6-Yonsei (5)	38	0.2	0.5	-5.6
Goddard-Yonsei (6)	36	-0.2	0.5	-5.6
Ferrier-MYJ (7)	39	0.0	0.5	-5.3
WDM6-MYJ (8)	35	-0.1	0.5	-6.8

Grid Configuration WFF

Dr. Watson spoke to Mr. Theodore Wilz at WFF about their modeling needs and the meteorological issues that affect their daily operations. Based on the information provided, Dr. Watson chose some preliminary domain configurations to test at the WFF. She ran different model configurations varying the dynamical core, grid spacing and domain size to determine the optimal configuration that allows for the largest domain size and highest resolution for a 24-hour forecast that can be run in under 1 hour. Figure 12 shows the domain she chose.

For more information contact Dr. Watson at watson.leela@ensco.com or 321-853-8264.

Table 10. Mean error of wind speed (m/s), direction (deg), temperature (°F), and dewpoint temperature (°F) from 1-7 August 2011 for Lin-Yonseil 2/0.67 km and 3/1 km configurations. The first number is the forecast value from the 2/0.67 km configuration and the second is from the 3/1 km configuration. Bold green values indicate the best performing model. Missing values indicate no sensor at that tower.

Tower Number	Wind Dir	Wind Spd	Temp	Dewpt
Tower 002	46/44	0.4/0.5	-1.9/-3.2	-0.4/-0.2
Tower 006	38/40	0.5/0.5	-0.2/-1.2	-2.3/-2.5
Tower 108	41/40	-0.4/-0.1	0.1/-1.3	
Tower 110	48/45	-0.5/-0.2	-0.3/-2.2	-0.9/-0.7
Tower 511	48/44	-0.5/0.3		
Tower 512	60/42	0.1/0.3	-2.1/-3.3	-4.2/-4.4
Tower 513	51/46	-0.2/-0.3		

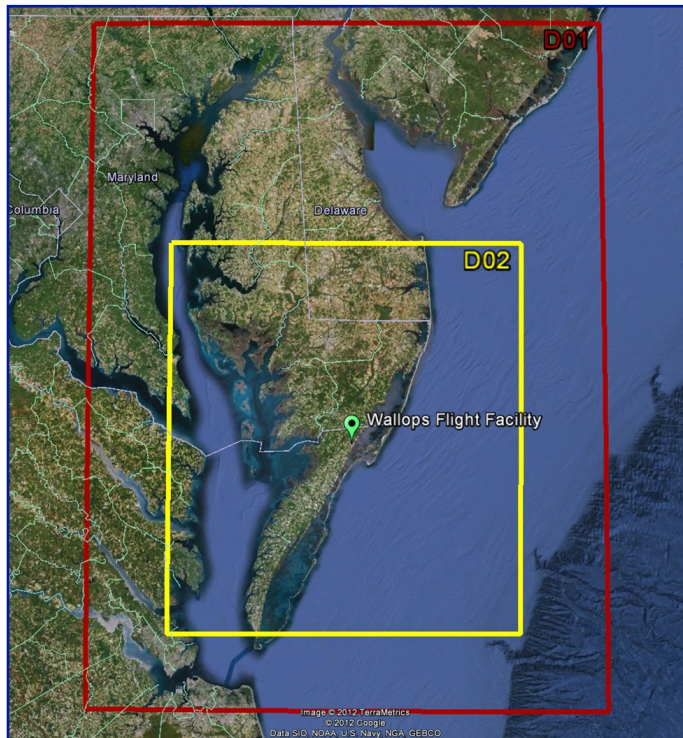


Figure 12. Domain configuration chosen for WFF centered over the Delmarva Peninsula. The outer domain (D01, red line) has a horizontal grid spacing of 4 km and the inner domain (D02, yellow line) has a grid spacing of 1.33 km.

AMU ACTIVITIES

AMU Chief's Technical Activities (Dr. Huddleston)

Dr. Huddleston attended the 92nd American Meteorological Society Annual Meeting in New Orleans, La., January 22-26. She also attended the 66th Interdepartmental Hurricane Conference in Charleston, S.C., March 5-9 with members of the 45 WS.

AMU Operations

Dr. Bauman and Dr. Watson attended the 92nd American Meteorological Society Annual Meeting in New Orleans, La., January 22-26. After 20 years of supporting the AMU, Mr. Wheeler retired on March 30. Ms. Schafer joined the AMU team full-time on April 2.

Dr. Watson was promoted from ENSCO Senior Scientist to ENSCO Staff Scientist effective 1 April.

Dr. Huddleston, Dr. Bauman and Ms. Shafer attended a NASA Accreditation Panel Briefing to assess the state of readiness of the AMU IT Security System. Following the briefing, the Accreditation Panel awarded the AMU IT System the Authority To Operate.

REFERENCES

- Bousquet, O., P Tabary, and J. du Châtelet, 2008: Operational multiple-Doppler wind retrieval inferred from long-range radial velocity measurements, *J. Appl. Meteor.*, **47**, 2929-2945.
- Lambert, W. and M. Wheeler, 2005: Objective lightning probability forecasting for Kennedy Space Center and Cape Canaveral Air Force Station. NASA Contractor Report CR-2005-212564, Kennedy Space Center, FL, 54 pp. [Available from ENSCO, Inc., 1980 N. Atlantic Ave., Suite 830, Cocoa Beach, FL, 32931, and <http://science.ksc.nasa.gov/amu/final-reports/objective-ltg-fcst-phase1.pdf>.]
- Lambert, W., 2007: Objective Lightning Probability Forecasting for Kennedy Space Center and Cape Canaveral Air Force Station, Phase II. NASA Contractor Report CR-2005-214732, Kennedy Space Center, FL, 57 pp. [Available from ENSCO, Inc., 1980 N. Atlantic Ave., Suite 830, Cocoa Beach, FL, 32931, and <http://science.ksc.nasa.gov/amu/final-reports/objective-ltg-fcst-phase2.pdf>.]
- TIBCO, 2010: TIBCO Spottfire S+® 8.2 Programmer's Guide, TIBCO Software Inc., Seattle, WA, 532 pp.
- Wilks, D. S., 2006: *Statistical Methods in the Atmospheric Sciences*. 2d ed. Academic Press, Inc., San Diego, CA, 467 pp.

LIST OF ACRONYMS

14 WS	14th Weather Squadron	MOC	Morrell Operations Center
30 SW	30th Space Wing	MSFC	Marshall Space Flight Center
30 WS	30th Weather Squadron	MYJ	Mellor-Yamada-Janjic PBL Scheme
45 RMS	45th Range Management Squadron	NAM	12-km North American Mesoscale model
45 OG	45th Operations Group	NCEP	National Centers for Environmental Prediction
45 SW	45th Space Wing	NLDN	National Lightning Detection Network
45 SW/SE	45th Space Wing/Range Safety	NMM	Non-hydrostatic Mesoscale Model (WRF)
45 WS	45th Weather Squadron	NOAA	National Oceanic and Atmospheric Administration
AFSPC	Air Force Space Command	NWS MLB	National Weather Service in Melbourne, FL
AFWA	Air Force Weather Agency	PAFB	Patrick Air Force Base
AMPS	Automated Meteorological Profiling System	PBL	Planetary Boundary Layer
AMU	Applied Meteorology Unit	Pers	1-Day Persistence
ARW	Advanced Research WRF	PoV	Probability of Violation
CCAFS	Cape Canaveral Air Force Station	PW	Precipitable Water
Climo	Daily Climatological Lightning Frequency	RH	Relative Humidity
CSR	Computer Sciences Raytheon	SI	Showalter Index
CT	Cross Totals	SMC	Space and Missile Center
ER	Eastern Range	SPoRT	Short-term Prediction Research and Transition Center
ESRL	Earth System Research Laboratory	SS	Brier Skill Score
FRProb	Flow Regime Lightning Probability	SWEAT	Severe Weather Threat Index
FSU	Florida State University	Tcl/Tk	Tool Command Language/Toolkit
GFS	Global Forecast System	TI	Thompson Index
GSD	Global Systems Division	TT	Total Totals
GUI	Graphical User Interface	USAF	United States Air Force
IRIS	Interactive Radar Information System	VAFB	Vandenberg Air Force Base
JSC	Johnson Space Center	VT	Vertical Totals
KSC	Kennedy Space Center	WFF	Wallops Flight Facility
KI	K Index	WRF	Weather Research and Forecasting
LCC	Launch Commit Criteria	WSR-88D	Weather Surveillance Radar 88 Doppler
LI	Lifted Index	XMR	CCAFS 3-letter identifier
MCO	Orlando International Airport 3-letter identifier		
MIDDS	Meteorological Interactive Data Display System		

The AMU has been in operation since September 1991. Tasking is determined annually with reviews at least semi-annually.

AMU Quarterly Reports are available on the Internet at <http://science.ksc.nasa.gov/amu/>.

They are also available in electronic format via email. If you would like to be added to the email distribution list, please contact Ms. Winifred Crawford (321-853-8130, crawford.winnie@ensco.com).

If your mailing information changes or if you would like to be removed from the distribution list, please notify Ms. Crawford or Dr. Lisa Huddleston (321-861-4952, Lisa.L.Huddleston@nasa.gov).

Distribution

NASA HQ/AA/ W. Gerstenmaier	NASA WFF/840.0/T. Wilz	HQ AFWA/A3/M. Surmeier	46 WS//DO/J. Mackey
NASA KSC/AA/R. Cabana	NASA DFRC/RA/E. Teets	HQ AFWA/A3T/S. Augustyn	46 WS/WST/E. Harris
NASA KSC/KT-C/J. Perotti	NASA LaRC/M. Kavaya	HQ AFWA/A3T/D. Harper	412 OSS/OSW/P. Harvey
NASA KSC/LX/P. Phillips	45 WS/CC/S. Cahanin	HQ AFWA/16 WS/WXE/ J. Cetola	412 OSS/OSWM/G. Davis
NASA KSC/LX/S. Quinn	45 WS/DO/B. Belson	HQ AFWA/16 WS/WXE/ G. Brooks	UAH/NSSTC/W. Vaughan
NASA KSC/LX-52/J. Amador	45 WS/ADO/W. Whisel	HQ AFWA/16 WS/WXP/ D. Keller	FAA/K. Shelton-Mur
NASA KSC/NESC-1/S. Minute	45 WS/DOR/M. McAleenan	HQ USAF/A30-W/R. Stoffer	FSU Department of Meteorology/H. Fuelberg
NASA KSC/NE-D2-A/P. Nicoli	45 WS/DOR/J. Smith	HQ USAF/A30-WX/T. Moore	ERAU/Applied Aviation Sciences/C. Herbster
NASA KSC/GP/S. Kerr	45 WS/DOR/M. Howard	HQ USAF/Integration, Plans, and Requirements Div/ Directorate of Weather/ A30-WX	ERAU/J. Lanicci
NASA KSC/GP/D. Lyons	45 WS/DOR/F. Flinn	NOAA "W/NP"/L. Uccellini	NCAR/J. Wilson
NASA KSC/GP/R. Mizell	45 WS/DOR/T. McNamara	NOAA/OAR/SSMC-I/J. Golden	NCAR/Y. H. Kuo
NASA KSC/GP/P. Nickolenko	45 WS/DOR/J. Tumbiolo	NOAA/NWS/OST12/SSMC2/ J. McQueen	NOAA/ESRL/GSD/S. Benjamin
NASA KSC/GP-B/J. Madura	45 WS/DOR/K. Winters	NOAA Office of Military Affairs/ M. Babcock	Office of the Federal Coordinator for Meteorological Services and Supporting Research/ R. Dumont
NASA KSC/GP-B/F. Merceret	45 WS/DOR/D. Craft	NWS Melbourne/B. Hagemeyer	Aerospace Corp/T. Adang
NASA KSC/GP-B/ L. Huddleston	45 WS/SY/M. Lewis	NWS Melbourne/D. Sharp	ITT/G. Kennedy
NASA KSC/GP-B/J. Wilson	45 WS/SYA/J. Saul	NWS Melbourne/S. Spratt	Timothy Wilfong & Associates/ T. Wilfong
NASA KSC/GP-G4/R. Brown	45 WS/SYR/W. Roeder	NWS Melbourne/P. Blottman	ENSCO, Inc./J. Stobie
NASA KSC/SA/R. Romanella	45 RMS/CC/V. Beard	NWS Melbourne/M. Volkmer	ENSCO, Inc./J. Clift
NASA KSC/SA/B. Braden	45 RMS/RMRA/R. Avvampato	NWS Southern Region HQ/"W/ SR"/S. Cooper	ENSCO, Inc./E. Lambert
NASA KSC/VA/A. Mitskevich	45 SW/CD/G. Kraver	NWS Southern Region HQ/"W/ SR3"/D. Billingsley	ENSCO, Inc./A. Yersavich
NASA KSC/VA-H/M. Carney	45 SW/SELR/K. Womble	NWS/"W/OST1"/B. Saffle	ENSCO, Inc./S. Masters
NASA KSC/VA-H1/B. Beaver	45 SW/XPR/R. Hillyer	NWS/"W/OST12"/D. Melendez	
NASA KSC/VA-H3/ P. Schallhorn	45 OG/CC/D. Sleeth	NWS/OST/PPD/SPB/P. Roohr	
NASA KSC/VA-2/C. Dovale	45 OG/TD/C. Terry	NSSL/D. Forsyth	
Analex Corp/Analex-20/ M. Hametz	CSC/M. Maier	30 OSS/OSWS/DO/J. Roberts	
NASA JSC/WS8/F. Brody	CSR 1000/S. Griffin	30 OSS/OSWS/M. Schmeiser	
NASA MSFC/EV44/B. Roberts	CSR 3410/C. Adams	30 OSS/OSWS/T. Brock	
NASA MSFC/EV44/R. Decker	CSR 3410/R. Crawford	30 SW/XPE/R. Ruecker	
NASA MSFC/EV44/H. Justh	CSR 3410/D. Pinter	Det 3 AFWAWXL/K. Lehneis	
NASA MSFC/ZP11/ G. Jedlovec	CSR 3410/M Wilson	NASIC/FCTT/G. Marx	
NASA MSFC/VP61/J. Case	CSR 4500/J. Osier		
NASA MFSC/VP61/G. Stano	CSR 4500/T. Long		
NASA WFF/840.0/R. Steiner	SLRSC/ITT/L. Grier		
NASA WFF/840.0/A. Thomas	SMC/OL-U/M. Erdmann		
	SMC/OL-U/T. Nguyen		
	SMC/OL-U/R. Bailey		
	SMC/CON/J. Gertsch		
	HQ AFSPC/A3FW/J. Carson		



NOTICE: Mention of a copyrighted, trademarked, or proprietary product, service, or document does not constitute endorsement thereof by the author, ENSCO, Inc., the AMU, the National Aeronautics and Space Administration, or the United States Government. Any such mention is solely for the purpose of fully informing the reader of the resources used to conduct the work reported herein.